

A novel modulation technique for FWM suppression in broadband coherent DWDM systems

G. P. KAUR^{a,*}, GURMEET KAUR^b, SANJAY SHARMA^a

^aThapar Institute of Engg. & Technology (Deemed University), Patiala (Punjab), India

^bPunjabi University, Patiala (Punjab), India

A novel QAM-PM modulation has been proposed for 112X10 Gbps system at 25 GHz spacing. At high data rates in narrow channel systems, FWM crosstalk limits the performance. Exploiting the phase dependence of FWM, we optimize the performance of a hybrid parametric amplifier using a phase shifted modified 4-QAM. Using the proposed system, a flat gain of more than 16 dB and gain ripple < 5 dB has been achieved without any gain flattening technique. The proposed modulation helps achieve higher spectral efficiency and a relatively flat gain in comparison to the conventional WDM system. Results show FWM suppression up to 5.8 dB.

(Received February 13, 2018; accepted November 29, 2018)

Keywords: High data rate, FWM crosstalk, suppression, Flat gain, Raman-FOPA

1. Introduction

Current optical communication systems are motivated by the quest to achieve higher transmission speed over longer distances. So, research in optical communication emphasizes the attainment of higher spectral efficiency (SE) with the use of advanced modulation formats. These high order modulation formats though are tolerant to linear transmission impairments as chromatic dispersion (CD) and polarization mode dispersion (PMD) but are vulnerable to the increased nonlinear crosstalk [1-3]. This places a stringent limitation of a higher optical signal to noise ratio (OSNR) [2] at the receiver using higher order modulation formats. This, in turn, necessitates the use of higher input launch powers. But high input power makes transmission more sensitive to fiber nonlinearities thereby limiting the reach of error-free transmission. Reduced channel spacing makes the effect of nonlinear crosstalk more severe in multichannel systems. Coherent-Wavelength Division Multiplexed (Co-WDM) systems have demonstrated reduced channel spacing comparable to the symbol rate per carrier without any crosstalk penalty [4-5]. In conventional WDM systems channel spacing equal to 1.2 times symbol rate per carrier using has been reported using 36-QAM [6]. But nonlinearities compensation remains a challenge to high performance in Co-WDM systems. To compensate for these fiber nonlinearities, use of fiber optical parametric amplifier (FOPA) via optical phase conjugation (OPC) has been demonstrated to be a potential candidate. OPC is generally implemented independently of the modulation format which makes it an attractive choice over complex compensation algorithms at the receiver [3, 7]. Also, FOPAs offer the advantages of low noise amplification and are tunable over a wide bandwidth [1].

Additionally, the recent research [8] shows that systems employing bi-directional distributed Raman amplification (DRA) effectively compensate for fiber nonlinearity through OPC in comparison to pure Erbium-doped Fiber amplifier(EDFA) amplified links. Coherent superimposed signal and generated idlers in Phase sensitive Fiber Optical Parametric amplifier (PS-FOPA) help cancel out the effect of fiber nonlinearities [9]. Application of Raman amplifiers for amplification in Dense Wavelength Division Multiplexed (DWDM) systems has been suggested in [10-11] employing Raman-EDFA cascade both for NRZ (Non-Return to Zero) [10] and differential phase shift keying (DPSK) modulation for flat gain, broadband amplification. Fu et al [12] have recently demonstrated the capabilities of Raman-phase sensitive FOPA(PS-FOPA) to enhance the gain of PS-FOPA over a wide band. The combination of Raman-based amplification and OPC scheme has been recently demonstrated for nonlinear distortions compensation using advanced modulation formats in high-speed WDM systems [7, 13-14]. From 70 dB peak small signal gain achieved in an 8 channel Dense Wavelength Division Multiplexed(DWDM) system [15] to gain of more than 20 dB over an extended gain bandwidth of 170 nm with gain ripple of less than 4 dB [16] has been demonstrated using varied configurations of Raman-parametric hybrid amplifiers. Research indicates Raman assisted FOPA employing Raman backward pumping in same length of Highly Non-Linear Fiber (HNLF) as used for FOPA [12, 17]. In [17], improved performance with Raman-FOPA (RA-FOPA) for WDM system has been achieved with a net gain of 20 dB and gain ripple of 1.9 dB for 10, 100 GHz spaced Distributed Feedback (DFB) lasers. Kaur et al[18] in previous work have demonstrated the wide gain amplification of 24.3 dB over a wide bandwidth of 220 nm using Raman amplifier cascaded with multi-section FOPA.

The flexibility in tuning the Raman-FOPA hybrid across any communication band has been established in previous research [15-20]. In this work, we extend the implementation of Raman-FOPA hybrid to high speed, coherent DWDM system. We propose a novel Quadrature Amplitude Modulation-Phase modulation (QAM-PM) modulated terabits capacity WDM system employing Raman-FOPA hybrid parametric amplifier and analyze the results for flat gain and Four Wave Mixing (FWM) generated idler suppression.

2. Simulation set up

The set up for QAM –PM modulation system comprises of 10 channel system extending from 190 THz to 190.225 THz at 25 GHz channel spacing. Each channel frequency is externally modulated by a QAM modulator with 4 bits per symbol. The QAM signal is then phase modulated by 45 degrees to create an additional phase modulation. This modulated signal is then launched into SMF of 50 km given to Raman amplifier followed by a single pump parametric amplifier.

The set up is as shown in Fig. 1. The use of QAM-PM modulation has been proposed in dispersion compensated system. The fiber used for Raman amplification serves as fiber for dispersion compensation as well. Raman amplifier employs backward pumping with the pump power of 450 mW at 1496 nm. This Raman amplified, dispersion compensated signal is then co-propagated with a high power parametric pump inside a small length of HNLF of 0.2 km for parametric amplification. The parametric pump uses the same power as Raman pump (450 mW) at a wavelength of 1577.4 nm.

The characteristics of HNLF and DCF used have been specified in Table 1. In a DWDM system as the number of channels ‘N’ increases, idlers generated due to FWM [21] increase as $M = [N^3 - N^2/2]$ and the average power of each generated idler falling on transmitted signal frequency estimation has been derived from [22] as:

$$P_{WDM} = (M/N)P_{ijk} \tag{1}$$

where P_{ijk} is given by:

$$P_{ijk} = \eta(1024\pi^6 \chi_{111}^2) \frac{d^2}{n^4 \lambda^2 c^2} \left(\frac{L_{eff}^2}{A_{eff}} \right) P_i P_j P_k e^{-\alpha N L} \tag{2}$$

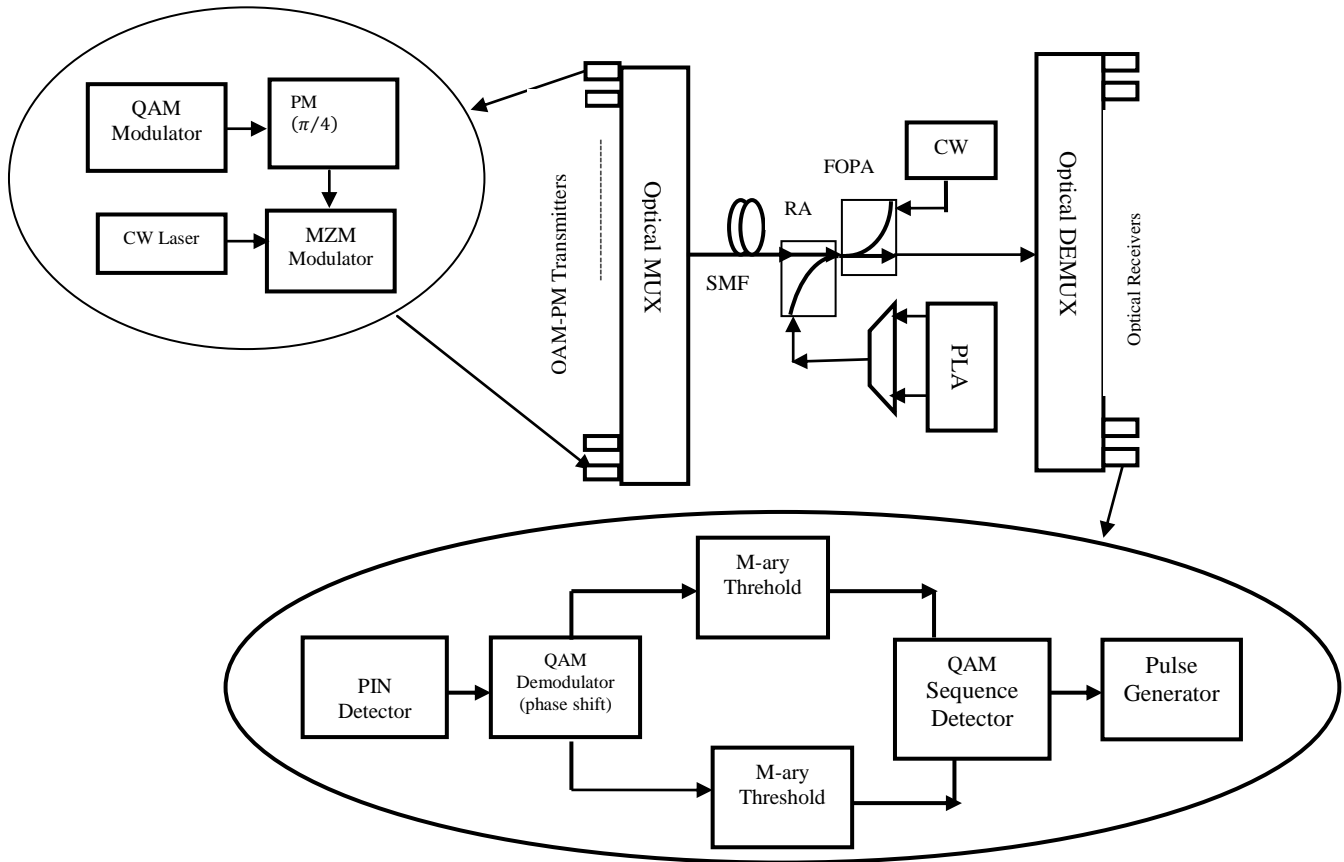


Fig. 1. Set up with QAM-PM modulated signals followed by Raman-FOPA for FWM suppression. PLA –Pump Laser Array, PM-Phase Modulator, MZM- Mach Zender Modulator, CW-Continuous Wave Laser

Now using QAM, each of the idler generated undergoes phase modulation with four different phases. A QAM signal $s(t)$ can be represented as [23]:

$$s_{QAM}(t) = s(t) \sqrt{(s_{mi}^2 + s_{mq}^2)} \exp j \left[\omega_c t + \tan^{-1} \left(\frac{s_{mi}}{s_{mq}} \right) \right] \quad (3)$$

where $\left[\omega_c t + \tan^{-1} \left(\frac{s_{mi}}{s_{mq}} \right) \right]$ represents the phase of QAM signals, s_{mi} and s_{mq} represent the inline and the quadrature components of the QAM signal.

In the proposed system, this signal $s_{QAM}(t)$ is further modulated by $\pi/4$ and the resultant signal as derived from (3) is:

$$s_{QAM}(t) = s(t) \sqrt{(s_{mi}^2 + s_{mq}^2)} \exp j \left[\omega_c t + \tan^{-1} \left(\frac{s_{mi}}{s_{mq}} \right) + \frac{\pi}{4} \right] \quad (4)$$

Table 1. Parameters used for HNLF - parametric amplifier and DCF in Raman amplifier

| Parameter | Value |
|-------------------------------------|--------------------|
| DCF length | 10 km |
| Dispersion (DCF) | -90 ps/km/nm |
| DCF attenuation | 0.5 dB/km |
| Effective area | 30 μm^2 |
| HNLF length | 0.2 km |
| HNLF effective area | 11 μm^2 |
| Dispersion (HNLF) | 2 ps/km/nm |
| Non-linear coefficient (γ) | 11.45 |
| HNLF attenuation | 0.8 dB/km |

It has been demonstrated that FWM generated idlers in WDM systems using higher order QAM, fall in the center of the transmission band [23]. As a result of additional phase modulation using proposed QAM-PM introduced the idlers generated due to FWM have random phases relative to each other, resulting in random varying powers of each idler. The additional phase shift has been introduced to exploit the phase dependence of FWM. The additional phase shift introduced after QAM would help change the relative phase of the signals and hence lead to the reduced power of generated idlers. This helps deviate the idler frequencies from the transmitted signal frequencies as well. Additionally, the type of fiber plays a significant role because of its dispersion characteristics. In case of SMF with ZDWL at 1550 nm effect of FWM in L-band frequencies is also less dominant than in C-band because of dispersion dependence of FWM.

In the proposed RAMAN-FOPA model RAMAN amplifier is cascaded directly with FOPA as shown in Fig. 1.

The gain of Raman amplifier is given as [21]:

$$G_{Raman} = 10 \log_{10} \left(\exp \left(g_R P \frac{L_{eff}}{A_{eff}} \right) - \alpha L \right) \quad (5)$$

where, g_R is Raman gain coefficient, P is pump power, L_{eff} is effective fiber length in Raman amplifier, A_{eff} is effective fiber area and α is fiber attenuation.

Gain of FOPA for the dual pump is given as [24]:

$$G_{FOPA} = 1 + \left\{ 2\gamma \frac{\sqrt{P_1 P_2}}{g} \sinh(gL) \right\}^2 \quad (6)$$

where, γ is non-linear coefficient, P_1, P_2 are pump powers, L is the length of fiber and g is parametric gain coefficient

$$g = \sqrt{4\gamma^2 P_1 P_2 - \left(\frac{k + \delta k}{2} \right)^2} \quad (7)$$

where, k is phase mismatch and given by:

$$k = \beta_2 \omega_c (\Delta\omega_s^2 - \Delta\omega_p^2) + \frac{1}{12} \beta_4 \omega_c (\Delta\omega_s^4 - \Delta\omega_p^4) + \gamma(P_1 + P_2) \quad (8)$$

$\omega_c = \frac{1}{2}(\omega_1 + \omega_2)$ for 2 pumps at P_1 and P_2 . For single pump FOPA $P_1=P_2=P$.

The gain expected of the used novel multi-pump Raman-FOPA cascade hybrid is:

$$G_{Hybrid} = G_{Raman} * G_{FOPA} \quad (9)$$

where, G_{Raman} is the individual gain of the Raman amplifier and G_{FOPA} is the individual gain of a single parametric amplifier

3. Results and discussions

We have implemented QAM-PM modulation in a dispersion compensated system employing a hybrid parametric amplifier. With 10 km of Raman fiber compensating the 50 km of SMF implemented the system is a partially compensated system. The results for gain variation in Fig. 2a shows improved gain achieved using QAM-PM modulation over a CW un-modulated WDM system at a high data rate of 112 Gbps. Both Raman and parametric pumps are at high power and total input power is also very high around 5mW for 10 channel system. With high input and pump powers nonlinearities are expected to have a pronounced impact specially FWM as the channel spacing between adjacent channels is 25 GHz and the data rate is very high. It is clearly observed from the gain variation of the proposed QAM-PM modulated system in Fig. 2a that QAM-PM offers higher and flat gain as compared to conventional WDM system. With QAM-PM modulated signals in a 10 channel WDM system maximum gain achieved is 16.95 and minimum gain is 12.08 dB giving the maximum ripple of 4.87 dB. On the other hand maximum gain in un-modulated CW WDM system is 16.34 dB and the minimum gain is 8.58 dB

giving ripple as high as 7.31dB. Also, the maximum gain improvement occurs at a frequency of 190.025 THz with $\Delta G = 3.61$ dB. This improvement in gain is attributed due to use of QAM-PM modulated signals as both systems employ Raman- parametric amplifier cascade.

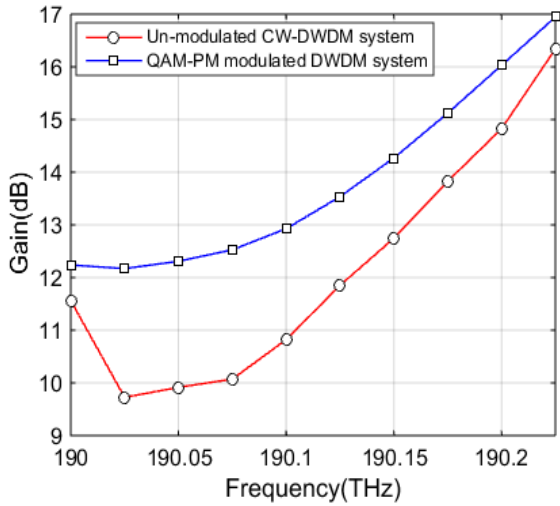


Fig. 2a. Gain Variations for QAM-PM modulated 10 Channel WDM system Vs CW WDM system

Observation of the OSNR results in Fig. 2b shows significant OSNR improvement using QAM-PM modulated system in comparison to conventional CW system. The blue curve indicates the OSNR for the proposed system as achieved at the output of Raman-FOPA cascade amplifier.

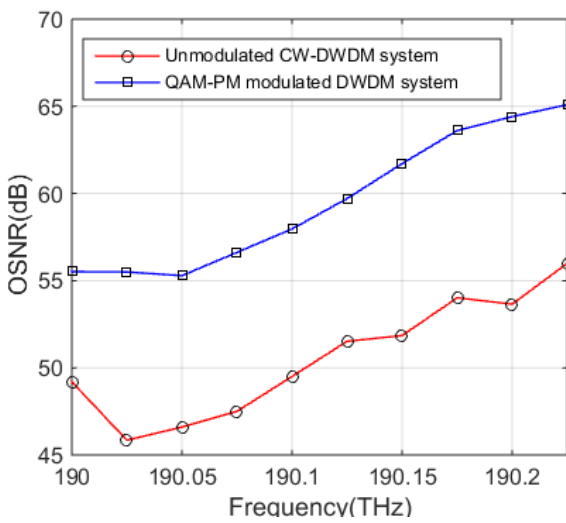


Fig. 2b. OSNR Variations for QAM-PM modulated 10 Channel WDM system Vs CW WDM system

In the proposed QAM-PM modulated WDM system maximum OSNR after traversing 50 km of dispersion compensated fiber is 65.01 dB against the maximum value of OSNR for the un-modulated system as 55.29 dB, almost 9 dB lesser.

For results of optical output power, in the proposed system the output power is much higher than the un-modulated system as observed from the results in Fig. 3a. Results in Fig. 3a establish significant FWM suppression achieved using QAM-PM modulation for transmitted signals when compared with CW un-modulated WDM system. To measure the amount of FWM suppression achieved we observe the output signal for QAM-PM modulated system as well as CW un-modulated WDM system in Fig. 3a and 3b. The results presented in the figure 3a and 3b are for the optical output power as received before giving input to the PIN detector. The output of QAM-PM modulated transmitted frequencies is significantly higher than that for the CW un-modulated WDM system. The FWM generated idlers falling at transmitted frequencies is significantly reduced using proposed modulation.

At the frequency of 190.05 THz FWM suppression achieved is highest using QAM-PM modulation is maximum. The achieved suppression is $\log_{10} \left(\frac{P_{QAM}}{P_{FWM}} \right)$ which gives the maximum value of 5.88 dB whereas at 190.1THz increase in signal power by 5.2 dB has been achieved. Observation of output power for QAM-PM Vs CW un-modulated WDM system also indicates better uniformity in the QAM-PM modulated output powers. For CW un-modulated WDM system at some frequencies, signal power falls drastically to even less than 0 dB. The valleys in the red curve of Fig. 3a for CW signals indicate these signal frequencies have suffered the most because of FWM as the generated idlers have fallen at these transmitted frequencies.

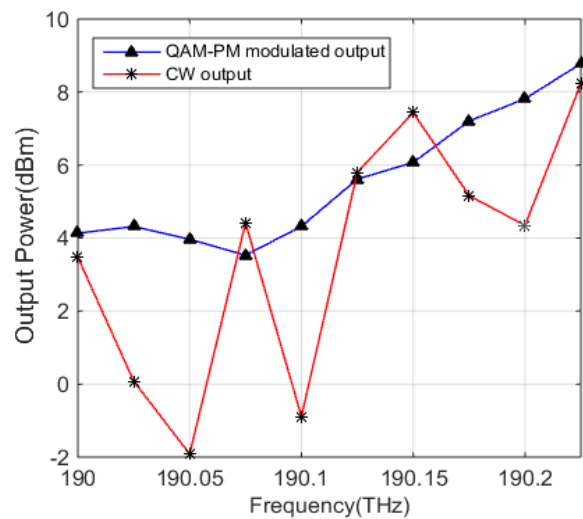


Fig. 3a. OSNR Variations for QAM-PM modulated 10 Channel WDM system Vs CW WDM system

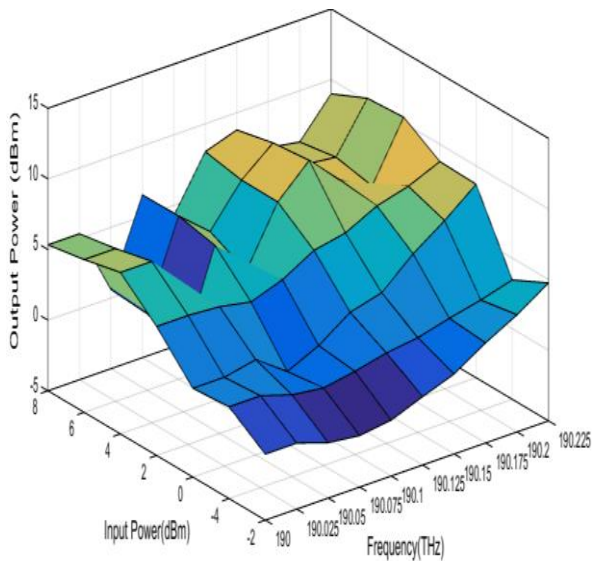


Fig. 3b. Mesh plot of output power variation of each QAM-PM modulated channel with varying input power

On the other hand observation of blue curve for QAM-PM modulated signal the decrease in signal power due to the direct imposition of FWM generated idlers at transmitted channel frequencies is far less.

Fig. 4 shows gain variations of the QAM-PM modulated system with varying total input powers. At the lower end for total input power of -4 dBm, the gain offered is highest at 18.87 dB. The minimum gain of 12.66 dB achieved at -4dB is the highest in comparison to higher input powers. As the total input power is increased to 0 dBm, the minimum gain falls, thereby increasing the gain ripple. The uniformity in gain curve can also be observed in red color curve to be the best for -4dBm input power.

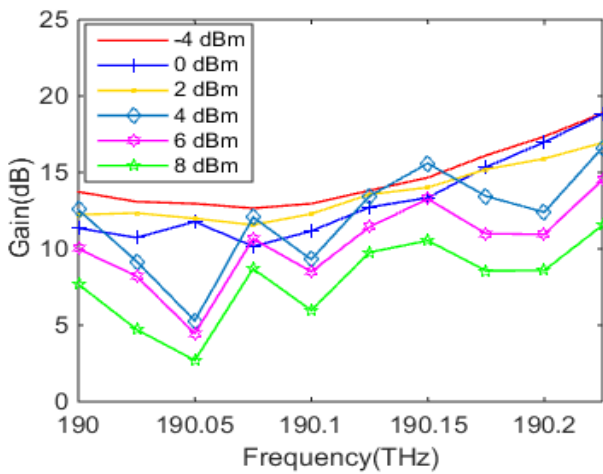


Fig. 4. Gain variations of QAM-PM modulated system With varying input powers of the system

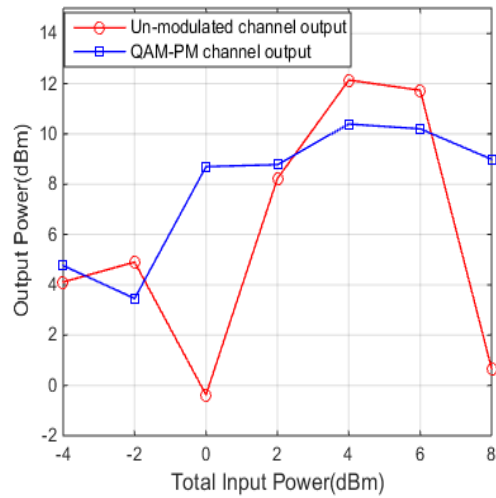


Fig. 5a. Output power variations with total input power for QAM-PM modulated system Vs CW WDM system

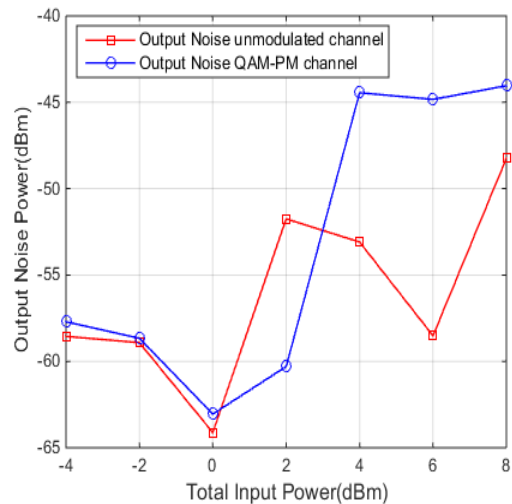


Fig. 5b. Output noise power variations with total input power for QAM-PM modulated system Vs CW WDM

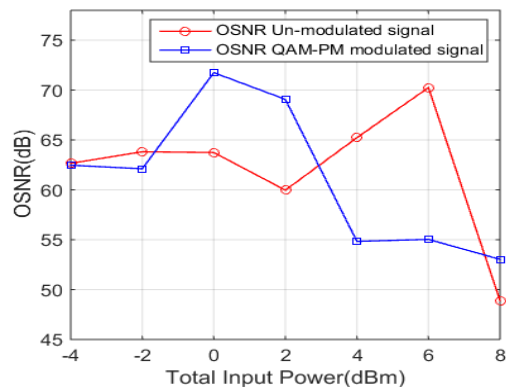


Fig. 6. OSNR variations with total input power for QAM-PM Modulated system Vs CW WDM system

With further increase in input power both peak gain and minimum gain decrease significantly giving very high gain ripple. For an input power of 8 dBm gain ripple is as high as 8.84 dB against the gain ripple of 6.21 dB achieved at an input power of -4dBm. This degradation in gain flatness and maximum peak gain with increasing high input powers is expected because of the increased nonlinearities in particular FWM. Results in Fig. 5a and 5b show the variations of output power and noise power generated for two systems under consideration for a channel at 190.225 THz. In Fig. 5a, for QAM-PM modulated signal there is an increase in output power with increasing input up to 6 dBm. After 6 dBm there is a slight fall in the output power with an increase in input power. On the other hand for CW signal in WDM system as the input power is increased from -4 dBm to -2 dBm there is negligible change in the output power. As input power is further increased there is a sharp decrease in signal power up to 0 dBm of input power. Beyond 0 dBm of input power the output starts increasing with an increase in input power and at 6 dBm there is again a steep fall in output signal power. So, with QAM-PM modulated signal output power increases with an increase in input power, unlike CW signal which shows sharp falling trends in the output.

Observing the results in Fig. 5b indicate a sharp increase in noise figure for both the QAM-PM modulated as well as CW signal with an increase in total input power. But at very high input powers of 4dBm and more QAM-PM shows very sharp increase in noise primarily due to increased non-linear crosstalk at high input powers. OSNR variations with total input power in Fig. 6 fall in line with the observations of Fig. 5a and 5b. As the dotted curve shows OSNR falls with increasing power. The fall in OSNR is onset for QAM-PM modulated signal at around 0 dBm and is maximum for 2 dBm to 4 dBm increase in power whereas for CW signal OSNR is stable with an increase in power up to 6 dBm which is higher than that for QAM-PM modulated signal. But at higher input powers of 6 dBm and more, the fall in OSNR of CW signal is very steep. This follows from the output signal variation of CW signal has a steep fall at 6 dBm power. Overall results show QAM-PM modulated signal shows better uniformity in the output signal, signal gain and OSNR variation in comparison to CW-WDM system at the high data rate of 112 Gbps in narrow spaced channels.

4. Results at receiver

The receiver of the proposed has been modeled as shown in the Fig. 1 inset of the receiver at de-multiplexer end. The signal from the de-multiplexer is received by PIN detector which includes shot noise, Amplified Spontaneous Emission (ASE) and thermal noise sources. The Electrical output signal is made to pass through an electrical filter to reduce noise. The filtered signal is then given as input to QAM demodulator. The outputs of I and Q channels from the demodulator to M-ary threshold detector. The plot of I and Q signals can be viewed on

constellation viewer. The Constellation as Sent for QAM-16 modeling using Gray coding is as shown in Fig. 7a with each of 16 symbols representing a unique combination of 4 bits.

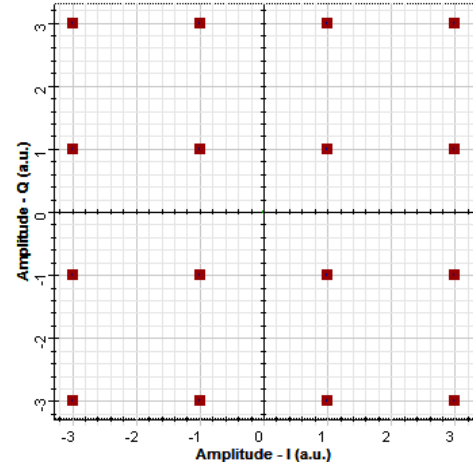


Fig. 7a. Input constellation for QAM-16

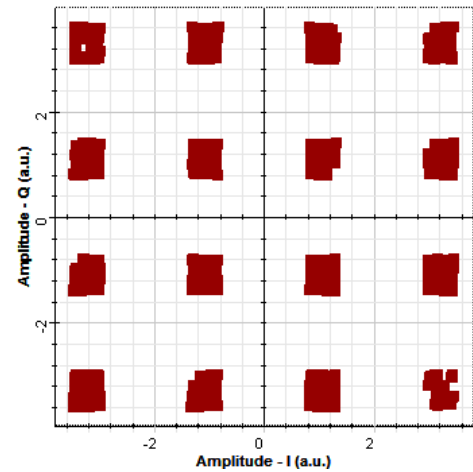


Fig. 7b. Received output constellation for QAM-16 at 800Mbps

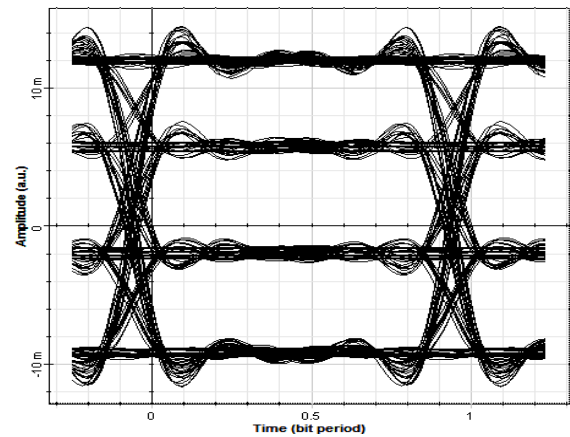


Fig. 7c. Received eye diagram for QAM-16 at 800Mbps

Under good conditions with Low data rates limited < 1Gbps received constellation is quite clear with amplitude

enough to be detected as shown in Fig. 7b and the corresponding eye diagram is shown in Fig. 7c. But as the data rate is increased to 112 Gbps at 25 GHz channel spacing, quality of the signal at the receiver is deteriorated due to phase noise and non-linear effects. Phase noise is a fundamental limitation to high data rate communication systems. The effect of phase noise is clearly observed in Fig. 8a where the shape of the QAM received symbols is degraded due to phase noise manifested as jitter. The corresponding eye diagram at the output is shown in Fig 8b which shows clear eye opening and achieves a BER of the order of 10^{-2} as Pre-FEC BER.

M-QAM has been investigated and established to perform well as compared to DPSK techniques [25] and has been found to scale well with the system complexity. But as the complexity of QAM is increased to more bits per symbol or sequence length of bits is increased, the non-uniform phase noise gives constellation diagrams, which are not discernable as shown in Fig. 9a and b for increased sequence lengths.

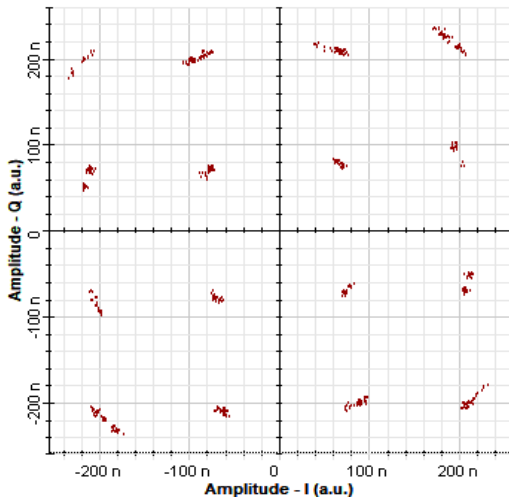


Fig. 8a. Received constellation diagram for QAM-16 at 112 Gbps for the channel at 190 THz

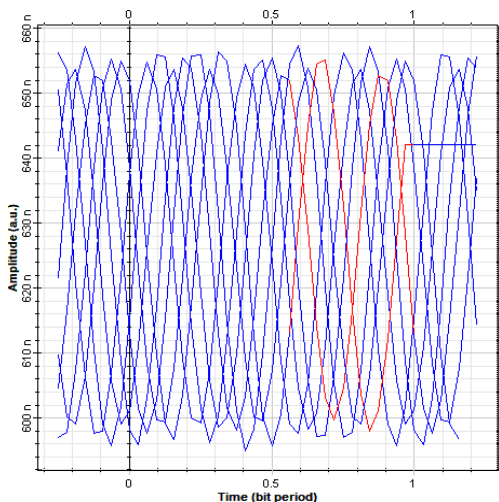


Fig. 8b. Received eye diagram for QAM-16 at 112 Gbps for the channel at 190 THz

This is attributed to the presence of phase noise which is contributed both laser line-widths as well as non-linear effects [26-27].

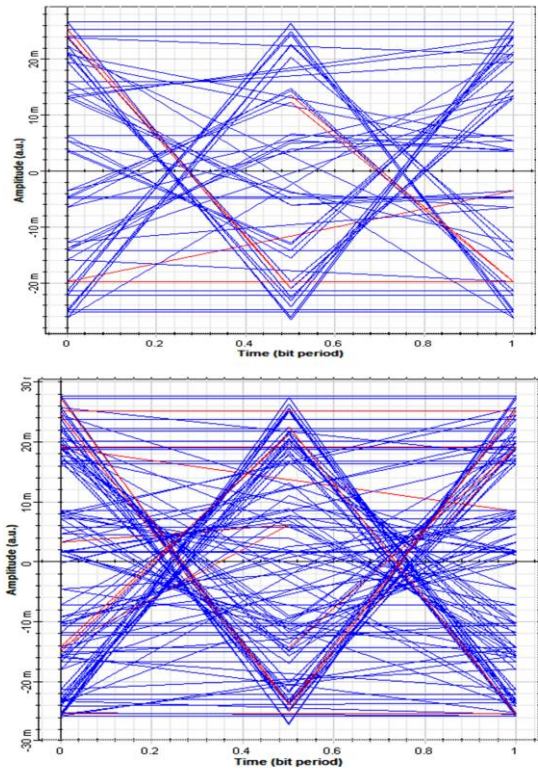


Fig. 9a and 9b showing eye diagrams for the increased number of bits per sequence 32 bit and 64 bits respectively of sample

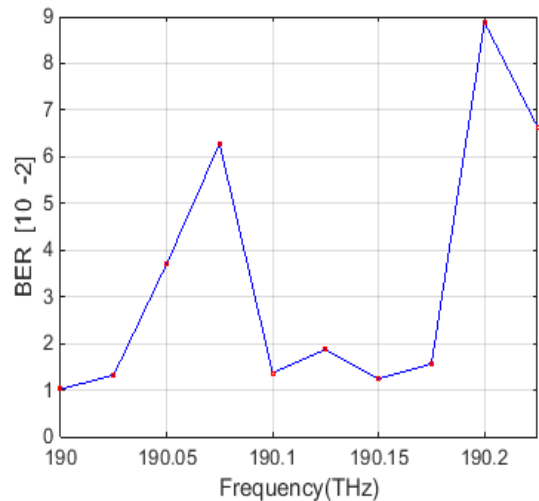


Fig. 9c. BER Vs Wavelength (nm) for proposed QAM-PM modulated system at 112 Gbps and 25 GHz channel spacing

Performance of a proposed coherent has been evaluated in terms of BER achieved at each channel as shown in Fig. 9c. A reasonable value of Pre-FEC BER of the order of 10^{-2} has been achieved which establishes the

capability of the proposed modulation coupled with multi-pump Raman and FOPA cascade as an efficient transmission configuration for 112 Gbps DWDM systems. The performance of proposed set up has been compared with the recent work in the field of parametric amplifiers,

in particular to hybrid configurations of Raman-FOPA either in Raman assisted parametric amplification or cascade configuration. Summarized results of the comparison have been tabulated in Table 2.

Table 2. Comparison of proposed with recent work

| Characteristic | 2015[22] | 2016 [28] | 2015 [17] | 2011 [29] | 2014 [16] | 2018 |
|--------------------------|----------------------------------|---|---------------------------------|------------------------------------|---------------------------------|---------------------------------|
| Amplifier Used | RA-FOPA | Phase Sensitive-FOPA | RA-FOPA | Multiple Raman pumps assisted FOPA | Tandem Configuration of RA-FOPA | Multiple Raman-FOPA Cascade |
| Bandwidth | 8 nm (1549.3 - 1542.1) nm C Band | 147 nm (S, C, U, and L –band) | 8 nm (1550.1- 1542.1) nm C band | 40 nm (1520- 1560) nm C band | 170 nm(1450- 1610)nm C+L Bands | 2 nm (1577.9 - 1575.9)nm L-band |
| Modulation Used | NRZ-QPSK | Phase Modulation | QPSK | PM | No modulation | QAM-PM |
| Transmission Rate | 58 Gbps | Electrical Frequency used 950 MHz | 58 Gbps | 2.5 Gbps | Not specified | 112 Gbps |
| No. of Channels | 10 | Tunable Laser used | 10 | 2 | 9 | 10 |
| Channel Spacing | 0.8 nm | Variable | 0.8 nm | 0.8 nm | 20 nm | 0.2 nm |
| Distance traveled | Only 0.2 Km of HNLf | No Distance traversed. | No Distance traveled | No distance Travelled | No distance Travelled | 50 km SMF +10 km DCF |
| Gain achieved | 20 dB | 9 dB | 20 dB | 18 dB | >20 dB | > 16 dB |
| Gain ripple | - | Equals to 9 dB as 0 dB considered as BW cut off | 1.9 dB | 1 dB | < 4dB | < 4.8 dB |

Table 2 shows most of the previous work of FOPAs and its hybrid with Raman amplifiers has been focused for C-band transmissions [16-17, 22, 29] except for the work presented in [28] which demonstrates the broadband capabilities of FOPA. Narrow channel spacing makes the system vulnerable to non-linear effects and establishing higher gain is difficult. Maximum gain in any configuration of Raman-FOPA hybrid has been demonstrated to be 20 dB at 100 GHz channel spacing but proposed the system in this work has a comparable gain of > 16 dB at the narrow channel spacing of DWDM. Additionally, all the previous work compared in Table 2 has evaluated the configuration from transmission between transmitter and receiver perspective, without taking into account the effect of channel length, channel noise and fiber dispersion. While determining the gain all these factors play a significant role. In the proposed system SMF has been employed over a transmission length of 50 km and yet maintain a comparable gain. Observations establish the proposed system as an effective alternative for DWDM system amplification without employing any gain flattening/compensating equipment making it a cost-effective solution to DWDM transmission.

5. Conclusion

We propose a novel modulation QAM-PM for high data rate narrow channel spaced WDM system employing

multi-pump Raman-FOPA as an in-line amplifier. Results achieved from set up implemented as 112 X10 Gbps, spaced at 25 GHz has shown better FWM suppression as compared to CW un-modulated WDM system. Due to FWM crosstalk suppression, the higher gain has been achieved using QAM-PM modulated signals employing the given set up. QAM-PM modulated signals shows better gain amplification when used in conjunction with the hybrid parametric amplifier as an inline amplifier.

Even the gain ripple has been significantly reduced for QAM-PM modulated system when compared with the system employing un-modulated CW-WDM signals.

References

- [1] J. Hansryd, P.A. Andrekson, M. Westlund, J. Li, P. Hedekvist, IEEE Journal on Selected Topics Quantum Electronics **8**(3), 506 (2002).
- [2] H. Hu, R. M. Jopson, A. H. Gnauck, M. Dinu, S. Chandrashekhar, C. Xie, S. Randel, IEEE Journal of Lightwave Technology **33**(7), 1286 (2015).
- [3] I. Sackey, F. Da Ros, T. Ritcher, R. Elschner, M. Jazayerifar, C. Meuer, C. Peucheret, K. Petermann, C. Schubert, The European Conference on Optical Communication (ECOC), Cannes, 1-3 (2014).
- [4] A. D. Ellis, F. C. G. Gunning, IEEE Photonics Technology Letters **17**, 504 (2005).

- [5] F. C. G. Gunning, T. Healy, X. Yang, A. D. Ellis, CLEO, Munich, Germany, paper CI8-5-FRI (2007).
- [6] X. Zhou, J. Yu, M. Huang, Y. Shao, T. Wang, L. Nelson, P. Magill, M. Birk, P. I. Borel, D. W. Peckham, R. Lingle, Optical Fiber Communication Conference, San Diego, CA, United States, 21st -25th March 2010, paper PDPB9 (2010).
- [7] I. Phillips, et al, Optical Fiber Communication conference, San Francisco, California, United States, 9th – 13th March 2014, Paper M3C.1.
- [8] P. Frascella, et al, IEEE Photonics Technology Letters **23**(14), 959 (2011).
- [9] S. L. Olsson, et al, Optical Fiber Communication Conference, San Francisco, California, United States, 9th – 13th March, (2014).
- [10] Simranjit Singh, R. S. Kaler, Fiber and Integrated Optics **31**(3), 208 (2012).
- [11] S. Singh, R. S. Kaler, Optical Engineering **52**(9), 96102 (2013).
- [12] X. Fu, X. Guo, C. Shu, Scientific Reports **6**, Article Number: 20180 (2016).
- [13] I. Sackey, et al., Optics Express **22**(22), 27381 (2015).
- [14] H. Hu, R. M. Jopson, A. H. Gnauck, M. Dinu, S. Chandrasekhar, S. X. Liu, C. Xie, M. Montoliu, S. Randel, C. J. McKinstrie, Optical Fiber Communication Conference, San Francisco, California, United States, 9th – 13th March, 2014.
- [15] S. H. Wang, P. K. A. Wai, OSA Conference on Lasers and Opto-Electronics, San Jose, 2010.
- [16] S. Peiris, N. Madamopoulos, N. Antoniadis, D. Richards, M. A. Ummy, R. Dorsinville, IEEE Journal of Lightwave Technology **32**(5), 939 (2014).
- [17] M. F. C. Stephens, I. D. Phillips, P. Rosa, P. Harper, N. J. Doran, Optics Express **23**(2), 902 (2015).
- [18] Gagan Kaur, G. Kaur, S. Sharma, Journal of Modern Optics **63**(9), 819 (2016).
- [19] Y. Akasaka, K. K. Y. Wong, M. C. Ho, M. E. Marhic, L. G. Kazovsky, presented at the OFC, Anaheim, CA, 2001, Paper WDD31-2 2001.
- [20] J. F. L. Freitas, M. B. Costa e Silva, S. R. Luthi, A. S. L. Gomes, Journal of Optics Communication **255**, (2005).
- [21] G. P. Agrawal, “Non-Linear Fiber Optics”, 4th Edition, Academic Press, (2007).
- [22] A. Redyuk, M. F. C. Stephens, N. J. Doran, Optics Express **23**(21), 27240 (2015).
- [23] Daniel Benedikovič, Ján Litvák, Milan Dado, Miroslav Markovič Jozef Dubovan, Proceedings SPIE 8697, 18th Czech-Polish-Slovak Optical Conference on Wave and Quantum Aspects of Contemporary Optics, 86972B (December 18, 2012).
- [24] E. Rotich, Proc for Sustainable Research and Innovation Conference **3**, 2011.
- [25] Fady I. El-Nahal, Photonics Letters of Poland **9**, 57 (2018).
- [26] X. Yi, W. Sheih, Y. Ma, IEEE Journal of Lightwave Technology **26**(10), 1309 (2008).
- [27] E. L. Efurumibe, A. D. Asiegbu, Journal of Information Engineering and Applications **2**(11), 35 (2012).
- [28] Rohit Malik, Aleš Kumpera, Magnus Karlsson, Peter A. Andrekson IEEE Photonics Technology Letters **28**(2), 175 (2016).
- [29] S. H. Wang, D. Wang, Chao Lu, T. Cheng, P. K. A. Wai, Journal of Lightwave Technology **29**(17), 2601 (2011).

*Corresponding author: preetkgagan@gmail.com